Basic Research in Cardiology (2019) 114:38
https://doi.org/10.1007/s00395-019-0745-y

ORIGINAL CONTRIBUTION

Mitochondrial bioenergetics links inflammation and cardiac contractility in endotoxemia

Tamara Antonela Vico[1,2] · Timoteo Marchini[1,3] · Santiago Ginart[4] · Mario Alejandro Lorenzetti[5] · Juan Santiago Adán Areán[2] · Valeria Calabró[1] · Mariana Garcés[1,3] · Mariana Cristina Ferrero[6] · Tamara Mazo[1,7] · Verónica D'Annunzio[1,7] · Ricardo J. Gelpi[1,7] · Daniel Corach[4] · Pablo Evelson[1,3] · Virginia Vanasco[1,2] · Silvia Alvarez[1,2]

Received: 18 December 2018 / Accepted: 30 July 2019 / Published online: 19 August 2019

Abstract

There is current awareness about the central role of mitochondrial dysfunction in the development of cardiac dysfunction in systemic inflammatory syndromes, especially in sepsis and endotoxemia. The aim of this work was to elucidate the mechanism that governs the link between the severity of the systemic inflammatory insult and mitochondrial function, analysing the consequences on heart function, particularly in cardiac contractile state. Female Sprague–Dawley rats were subjected to low-grade endotoxemia (i.p. injection LPS 0.5 mg kg^{-1} body weight) and severe endotoxemia (i.p. injection LPS 8 mg kg^{-1} body weight) for 6 h. Blood NO, as well as cardiac TNF-α and IL-1β mRNA, were found increased as the severity of the endotoxemia increases. Cardiac relaxation was altered only in severe endotoxemia, although contractile and lusitropic reserves were found impaired in both treatments in response to work-overload. Cardiac ultrastructure showed disorientation of myofibrillar structure in both endotoxemia degrees, but mitochondrial swelling and cristae disruption were only observed in severe endotoxemia. Mitochondrial ATP production, O_2 consumption and mitochondrial inner membrane potential decreases were related to blood NO levels and mitochondrial protein nitration, leading to diminished ATP availability and impairment of contractile state. Co-treatment with the NOS inhibitor L-NAME or the administration of the NO scavenger c-PTIO leads to the observation that mitochondrial bioenergetics status depends on the degree of the inflammatory insult mainly determined by blood NO levels. Unravelling the mechanisms involved in the onset of sepsis and endotoxemia improves the interpretation of the pathology, and provides new horizons for novel therapeutic targets.

Keywords Mitochondrial bioenergetics · Cardiac dysfunction · Systemic inflammation · Endotoxemia · Nitric oxide

Abbreviations

ATP	Adenosine triphosphate
ADP	Adenosine diphosphate

Electronic supplementary material The online version of this article (https://doi.org/10.1007/s00395-019-0745-y) contains supplementary material, which is available to authorized users.

✉ Virginia Vanasco
vvanasco@ffyb.uba.ar

✉ Silvia Alvarez
salvarez@ffyb.uba.ar

[1] Instituto de Bioquímica y Medicina Molecular (IBIMOL), Facultad de Farmacia y Bioquímica, Universidad de Buenos Aires-CONICET, Buenos Aires, Argentina

[2] Departamento de Química Analítica y Fisicoquímica, Facultad de Farmacia y Bioquímica, Cátedra de Fisicoquímica, Universidad de Buenos Aires, Junín 956, C1113AAD, Buenos Aires, Argentina

[3] Departamento de Química Analítica y Fisicoquímica, Facultad de Farmacia y Bioquímica, Cátedra de Química General e Inorgánica, Universidad de Buenos Aires, Buenos Aires, Argentina

[4] Servicio de Huellas Digitales Genéticas, Facultad de Farmacia y Bioquímica, Universidad de Buenos Aires, Buenos Aires, Argentina

[5] División Patología, Instituto Multidisciplinario de Investigaciones en Patologías Pediátricas (IMIPP), CONICET-GCBA, Hospital de Niños Ricardo Gutiérrez, Buenos Aires, Argentina

[6] Instituto de Estudios de la Inmunidad Humoral (IDEHU), Facultad de Farmacia y Bioquímica, Universidad de Buenos Aires-CONICET, Buenos Aires, Argentina

[7] Departamento de Patología, Instituto de Fisiopatología Cardiovascular, Facultad de Medicina, Universidad de Buenos Aires, Buenos Aires, Argentina

BSA	Bovine serum albumin
c-PTIO	2-(4-Carboxyphenyl)-4,4,5,5-tetramethylimidazoline-1-oxyl-3-oxide potassium salt
DAF	4,5-Diaminofluorescein
DCF	2′,7′-Dichlorofluorescein
ISO	Isoproterenol
L-NAME	N_{ω}-nitro-L-arginine methyl ester hydrochloride
LPS	Lipopolysaccharide
MM	Mitochondrial membranes
NADH	Nicotinamide adenine dinucleotide
NO	Nitric oxide
NO_x^-	Nitrite/nitrate
$ONOO^-$	Peroxynitrite
PMN	Polymorphonuclear leukocytes
RCR	Respiratory control ratio
ROS	Reactive oxygen species
TNF-α	Tumor necrosis factor

Introduction

Sepsis is defined as a life-threatening organ dysfunction caused by a deregulated host response to infection [1]. Sepsis and severe endotoxemia, caused by the presence of high levels of lipopolysaccharide (LPS) in the blood, are characterized by the massive increase of nitric oxide (NO) and inflammatory cytokines in biological fluids, systemic damage in the vascular endothelium, and impaired tissue respiration despite adequate O_2 supply [2]. During an acute inflammatory response, an initial pro-inflammatory phase is characterized by neutrophil recruitment and production of pro-inflammatory cytokines, such as TNF-α, IL-1β, and IL-6, and is followed by an anti-inflammatory phase with compensatory induction of anti-inflammatory cytokines, such as IL-10 [3]. If the pro-inflammatory scenario fails to resolve, it evolves to a persistent state of low-grade inflammation [4]. In this context, there has been growing interest in metabolic endotoxemia where a low and persistent increase of circulating LPS is associated with metabolic derangements [5, 6]. This situation can be found in states of obesity, type 2 diabetes and aging [7, 8].

Myocardial dysfunction is a well-recognized manifestation in systemic inflammatory syndromes. Septic related cardiomyopathy is multifactorial, and one of the main proposed mechanisms for the pathogenesis of myocardial dysfunction supports a prominent role for functional rather than anatomical abnormalities. However, attempts to reduce the high mortality rate in septic patients by manipulating functional alterations have provided limited success [9–12]. Thus, integrated and more specific studies are needed to unravel the importance and hierarchy of the cellular and biochemical processes occurring in the heart.

There is current awareness about the central role of mitochondrial dysfunction in the development of heart failure in this syndrome. Mitochondria provide energy to the cell through the synthesis of ATP by F_0–F_1 ATP synthase. Consequently, impaired ATP production may result in bioenergetic dysfunction and cardiac failure. Mitochondrial ATP levels have been suggested to be related to the patient's outcome [13, 14]. Moreover, systemic inflammatory syndromes may occur with cytopathic hypoxia; although O_2 tension in the organ may be normal, mitochondria fail to properly produce ATP from the consumed O_2 [15]. Dysfunctional mitochondria may produce increased levels of reactive O_2 species (ROS) that can interact with circulating NO; thus, producing peroxynitrite ($ONOO^-$), a powerful oxidant leading to tissue damage and organ failure. During experimental sepsis, $ONOO^-$, rather than NO per se, has been shown to impair muscle contractility by its ability to oxidize proteins, perturb calcium flux, and inhibit the electron transport chain by nitrosylation or nitration of mitochondrial respiration complexes [16, 17]. In a previous work of this laboratory, in an animal model of endotoxemia, mitochondria dysfunction was evidenced as well as changes in mitochondrial dynamics (including mitochondrial biogenesis, fission and autophagy). The fact that the latter mechanisms have been activated in this pathophysiological condition, suggests an attempt to compensate mitochondrial dysfunction; thus, revealing the importance of maintaining mitochondrial function during endotoxemia [18].

In this work, we used two doses of LPS to generate two different endotoxemia degrees (low-grade and severe). Taking into account the increasing evidence suggesting that mitochondria have a crucial role in the development of sepsis and endotoxemia, the aim of this work was to elucidate the mechanism that governs the link between the severity of the systemic inflammatory insult and mitochondrial function, analysing consequences on ventricular function, particularly in cardiac contractile state. The obtained results including the in vivo co-treatment with the NOS inhibitor L-NAME or the administration of the NO scavenger c-PTIO, allowed us to propose that the inflammatory insult mainly characterized by NO blood levels, has a causal relationship with decreased mitochondrial bioenergetics, and ultimately cardiac contractile state. To our knowledge, no studies have been carried out on mitochondrial function, cardiac function, and systemic inflammatory response in vivo integrated into the same animal model modulating NO levels by different approaches.

Methods

Detailed methods can be found in the Supplementary material online.

Experimental model

Animal experiments were approved by the Animal Care and Research Committee of the School of Pharmacy and Biochemistry, University of Buenos Aires (CICUAL; Exp. 0054032/15), and strictly followed the NIH guidelines. Also, practical guidelines on experimental studies in cardioprotection were followed [19]. In this study, Female Sprague–Dawley rats (45 ± 5 days old) were obtained from the Animal Facility of the School of Pharmacy and Biochemistry of the University Buenos Aires and were housed under standard conditions of light, temperature and humidity, with unlimited access to water and pelleted rodent food. Intraperitoneal injection of LPS is an extensively used model of endotoxemia [20, 21]. Moreover, it has been previously shown that this model induces cardiac alterations that closely resemble the ones observed in human sepsis [22]. To induce low-grade endotoxemia, animals were i.p. injected with LPS (serotype 026:B6 from *Escherichia coli*) 0.5 mg kg^{-1} of body weight, while to induce severe endotoxemia, rats were i.p. injected with LPS 8 mg kg^{-1} of body weight. Control animals received an equivalent volume of vehicle. After 6 h of treatment, animals were euthanized in a CO_2 chamber, and the heart and blood samples were collected for analysis.

When necessary, and with the aim to in vivo modulate NO levels, L-NAME (NOS inhibitor) or c-PTIO (NO scavenger) were used in each of the tree experimental groups previously described. When L-NAME was used, animals were i.p. co-injected with vehicle/LPS plus L-NAME 20 mg kg^{-1} of body weight [23]. When c-PTIO was used, animals were i.v. injected with c-PTIO 1.7 mg kg^{-1} of body weight at 60, 90 and 120 min after injection with vehicle/LPS [24, 25].

Cytokines quantification

The content of TNF-α and IL-6 in plasma samples were measured by sandwich ELISA using paired cytokine-specific mAbs, according to manufacturer's instructions (BD Biosciences OptEIA™ set, NJ, US). Results were expressed as pg mL^{-1} for plasma.

Flow cytometry assessment of intravascular leukocyte activation

Leukocyte isolation was performed as described earlier [26, 27]. To analyze leukocyte respiratory burst activity and intracellular NO production, isolated leukocytes were loaded with 10 µM 2′,7′-dichlorofluorescein (DCF) diacetate or 10 µM 4,5-diaminofluorescein (DAF-2) diacetate, and acquired on a FACSCalibur flow cytometer (Becton–Dickinson, NJ, US). See Supplementary material online for the detailed procedure.

NO-haemoglobin (NO-Hb) in blood by electron paramagnetic resonance (EPR)

Rats were anesthetized in a CO_2 chamber; blood was obtained by cardiac puncture, and immediately stored at 77 K (liquid N_2) until analyzed. EPR spectra were obtained at 77 K in a Bruker spectrometer (Bruker ECS106, Karlsruhe, Germany) with an ER 4102ST cavity. Detailed scan parameters are included in the Supplementary material online.

Nitrite/nitrate content

Nitrite/nitrate content in plasma or left ventricle tissue homogenate (Supplementary material online) was measured by performing a modified Griess reaction [28]. Briefly, samples were deproteinized through ethanol precipitation. Afterwards, deproteinized samples were incubated with 8 mg mL^{-1} vanadium(III) chloride (VCl_3) for 30 min at 37 °C to reduce nitrate to nitrite. The detection of nitrite was performed by the Griess reaction. Results were expressed as µM NO_x^- or nmol NO_x^- mg $protein^{-1}$.

Isolated heart perfusion

Animals were anesthetized by an i.p. injection of sodium pentobarbital (150 mg kg^{-1} body weight) and sodium heparin (500 UI kg^{-1} body weight). Hearts were excised and placed in a perfusion system according to the Langendorff technique, as previously described [29]. See Supplementary material online for extended procedure. Contractile state was evaluated as left ventricular developed pressure (LVDP), and isovolumic relaxation (lusitropism) was analysed as the time required for the left ventricular pressure to fall up to 50% from the peak of LVDP (t_{50}) [30], before and after a β-adrenergic stimulus through the addition of 1 µM isoproterenol (ISO) to the perfusion line [31, 32].

Quantification of cytokines mRNA in the heart by RT-qPCR

Total RNA was purified from frozen heart samples with ReliaPrep™ RNA Tissue Miniprep System kit (Promega, Madison, WI, US) according to manufacturer's instructions. The Improm-II™ Reverse Transcription System (Promega, Madison, WI, US) was used to synthesize random hexamer-primed cDNA. Targets of interest were amplified by PCR using the primers described in Table 1. PCR primers were designed using the online IDT PrimerQuest Tool (https://www.idtdna.com/Primerquest/Home/Index). For relative quantitation of TNF-α and IL-1β, the β-actin housekeeping

Table 1 Primers for RT-qPCR

mRNA targets	Sense	Antisense
TNF-α	5′-CAAATGGGCTCCCTCTC-3′	5′-CTACGGGCTTGTCACTC-3′
IL-1β	5′-AGCTACCTATGTCTTGCC-3′	5′-GGAACATCACACACTAGC-3′
IL-10	5′-CATACTGCTGACAGATTCC-3′	5′-TGCTCCTTGATTTCTGG-3′
β-actin	5′-CTATGAGCTGCCTGACG-3′	5′-TTCATGGATGCCACAGG-3′

gene was used as an endogenous control. Extended procedure is presented in Supplementary material online.

Histology

Myocardial tissue portions were formalin-fixed and paraffin embedded. Three micrometer tissue slides were then stained with the hematoxilin-eosin technique. Details are included in the Supplementary material online.

Transmission electron microscopy (TEM) of left ventricle tissue

Left ventricle tissue processing was performed as described before [18]. Briefly, tissue was cut into 1 mm^3 cubes, and fixed with 2.5% glutaraldehyde in phosphate medium pH 7.4. After postfixation with 1% osmium tetroxide in 0.1 M phosphate buffer, tissue was contrasted with 5% uranylacetate, dehydrated, and embedded in Durcupan resin (Fluka AG, Switzerland). Ultrathin sections were cut and then observed with a Zeiss EM 109 transmission electron microscope (Oberkochen, Germany); digital images were captured with a CCD GATAN ES1000 W camera (CA, USA).

Mitochondrial isolation and preparation of mitochondrial membranes

Animals were anaesthetized, and hearts were immediately excised. Heart mitochondrial purified fractions were obtained as described earlier [18, 33] by differential centrifugation, with previous digestion with 2.5 UI mL^{-1} type XXIV bacterial proteinase (for mitochondrial preparation details see Supplementary material online). Mitochondrial membranes (MM) were obtained by freezing and thawing mitochondria three times and homogenizing by passage through a 29G hypodermic needle [34]. Protein concentration was measured by the Lowry assay using BSA as a standard [35].

Mitochondrial O_2 consumption

Mitochondrial O_2 consumption was measured in freshly isolated mitochondria using a Clark-type O_2 electrode for high-resolution respirometry (Hansatech Oxygraph, Hansatech Instruments Ltd., Norfolk, UK). Resting respiration state (state 4) was measured in the presence of 2 mM malate and 5 mM glutamate as substrates, and then followed by the addition of 1 mM ADP, an active respiration state (state 3) was obtained. Respiratory control ratio (RCR) was calculated as the ratio between state 3 and state 4 respiration rates [36]. See Supplementary material online for the detailed procedure.

Mitochondrial ATP production rate and P/O ratio

ATP production rate was measured in isolated mitochondria using the luciferin/luciferase assay in a microplate reader (Varioskan® LUX, Thermo Scientific, MA, US). The efficiency of the oxidative phosphorylation process (P/O ratio), was calculated as the number of phosphorylated ADP molecules per O_2 atom (ATP production rate/state 3 O_2 consumption rate) [37]. See Supplementary material online for the detailed procedure.

Mitochondrial membrane potential ($\Delta\Psi_m$)

Mitochondrial inner membrane potential ($\Delta\Psi_m$) was analysed in freshly isolated mitochondria by flow cytometry using 120 nM of the potentiometric cationic probe 3,3′-dihexyloxacarbocyanine iodide ($DiOC_6$) as previously described [38]. The 10-N-nonyl acridine orange (NAO) probe was used to selectively stain mitochondria and to evaluate their purity, due to its ability to selectively bind to cardiolipin at the inner mitochondrial membrane [39]. Mitochondria selected population was 95% NAO positive. Total depolarization induced by 2 µM m-CCCP was used as a positive control. Extended procedure is presented in Supplementary material online.

Respiratory chain complexes activities

NADH-cytochrome *c* reductase (complex I–III) and succinate cytochrome *c* reductase (complex II–III) activities were measured by a colorimetric assay following cytochrome c^{3+} reduction at 550 nm ($\varepsilon = 19.6$ mM^{-1} cm^{-1}) in MM. Cytochrome oxidase activity (complex IV) was assayed spectrophotometrically at 550 nm by following the oxidation rate of 50 mM cytochrome c^{2+} in MM [40, 41]. See Supplementary material online for the detailed procedure.

Mitochondrial H_2O_2 production rate

To study ROS generation from freshly isolated mitochondria, H_2O_2 production was measured by fluorescence spectroscopy using the Amplex Red/horseradish peroxidase (HRP) system [42] using 2 mM malate and 5 mM glutamate as substrates. Extended procedure is presented in Supplementary material online.

Statistical analysis

Results were expressed as mean values ± SEM and represent the mean of independent experiments. At least five animals per treatment were used, and experiments were run in triplicate for each independent experiment. ANOVA followed by the post hoc Tukey's test was performed to analyse differences between experimental groups. Statistical significance was considered at $p < 0.05$.

Results

Pro-inflammatory response increased with the severity of endotoxemia

To analyse systemic innate inflammatory response in low-grade and severe endotoxemia, blood total leukocyte count was determined and found significantly decreased by 51% in the severe endotoxemia group compared to the control group ($p < 0.05$) (Table 2). Moreover, differential WBC count showed that, in both groups of LPS-treated animals, neutrophil percentage in peripheral blood increased by 58% ($p < 0.05$). To evaluate intravascular activation of innate immune cells, leukocyte ROS and NO production were assessed by flow cytometry (Fig. 1a). Quantification of DCF fluorescence showed an increase of 88% in ROS production in the low-grade endotoxemia group, and of 94% in the severe endotoxemia group compared to control animals ($p < 0.05$) (Fig. 1b). NO production by PMN leukocytes was analysed by DAF-2 fluorescence quantification, showing an increase in low-grade and severe endotoxemia groups of 42% ($p < 0.05$) and 60% ($p < 0.01$) respectively (Fig. 1c). This observation indicates enhanced PMN activation and NO production in LPS-treated animals compared to control animals.

Blood NO levels were measured by two different approaches to characterize the degree of the inflammatory response. Total blood NO was measured by EPR by the direct formation of the mononitrosyl-hemoglobin adduct (Hb-NO) and found increased by sixfold in low-grade animals compared to control animals, whereas in severe endotoxemia, a 18-fold increase was observed compared to the control ($p < 0.05$) (Fig. 1d, e). Moreover, as a certain amount of NO may react with oxyhemoglobin and thus being oxidized to nitrate [43], total plasma nitrite/nitrate content was analysed. As shown in Fig. 1f, a fivefold ($p < 0.01$) and 13-fold ($p < 0.0001$) increase in NO_X^- levels in low-grade and severe endotoxemia was found. Interestingly, in the severe endotoxemia group, a threefold increase of nitrite/nitrate levels compared to low-grade endotoxemia was observed ($p < 0.0001$). These results indicate that blood NO concentration is related to the severity of the inflammatory insult. Finally, pro-inflammatory TNF-α and IL-6 plasma content were measured (Fig. 1g). Plasma levels of both cytokines showed a tendency to increase with the severity of the endotoxemia, although significant differences were observed only in severe endotoxemia compared to control animals ($p < 0.05$).

Cardiac function and inflammation depend on the degree of endotoxemia

Regarding cardiac contractile state, LVDP was not altered among the different experimental groups in basal conditions (Fig. 2a). However, after a β-adrenergic stimulus with ISO, a minor increase in LVDP (expressed as %ΔLVDP) was observed in LPS-treated animals compared with control animals. As shown in Fig. 2b, control animals showed an increase of 39% in LVDP after ISO perfusion, while %ΔLVDP was only 21% in low-grade, and 20% in severe endotoxemia ($p < 0.05$). These results indicate an impaired contractile reserve in both treated groups. Moreover, isovolumetric relaxation was evaluated through t_{50}, and although no changes were observed in ventricular relaxation for low-grade endotoxemic animals, an attenuated t_{50} was found in the severe endotoxemia group compared to the

Table 2 WBC count and differential count in control, low-grade and severe endotoxemia

	Control	Low-grade endotoxemia	Severe endotoxemia
Total white cell count	3961 ± 507	4296 ± 996	1999 ± 307*
Neutrophils	673 ± 156 (17%)	2696 ± 507* (58%)	2502 ± 531* (57%)
Lymphocytes	3293 ± 522 (82%)	1740 ± 340* (40%)	1787 ± 323* (41%)
Monocytes	133 ± 24 (3%)	107 ± 44 (2%)	67 ± 40 (1%)
Eosinophils	0 (0%)	0 (0%)	0 (0%)
Basophils	0 (0%)	0 (0%)	0 (0%)

*$p < 0.05$ as compared to control group by ANOVA-Tukey's test ($n = 8$)

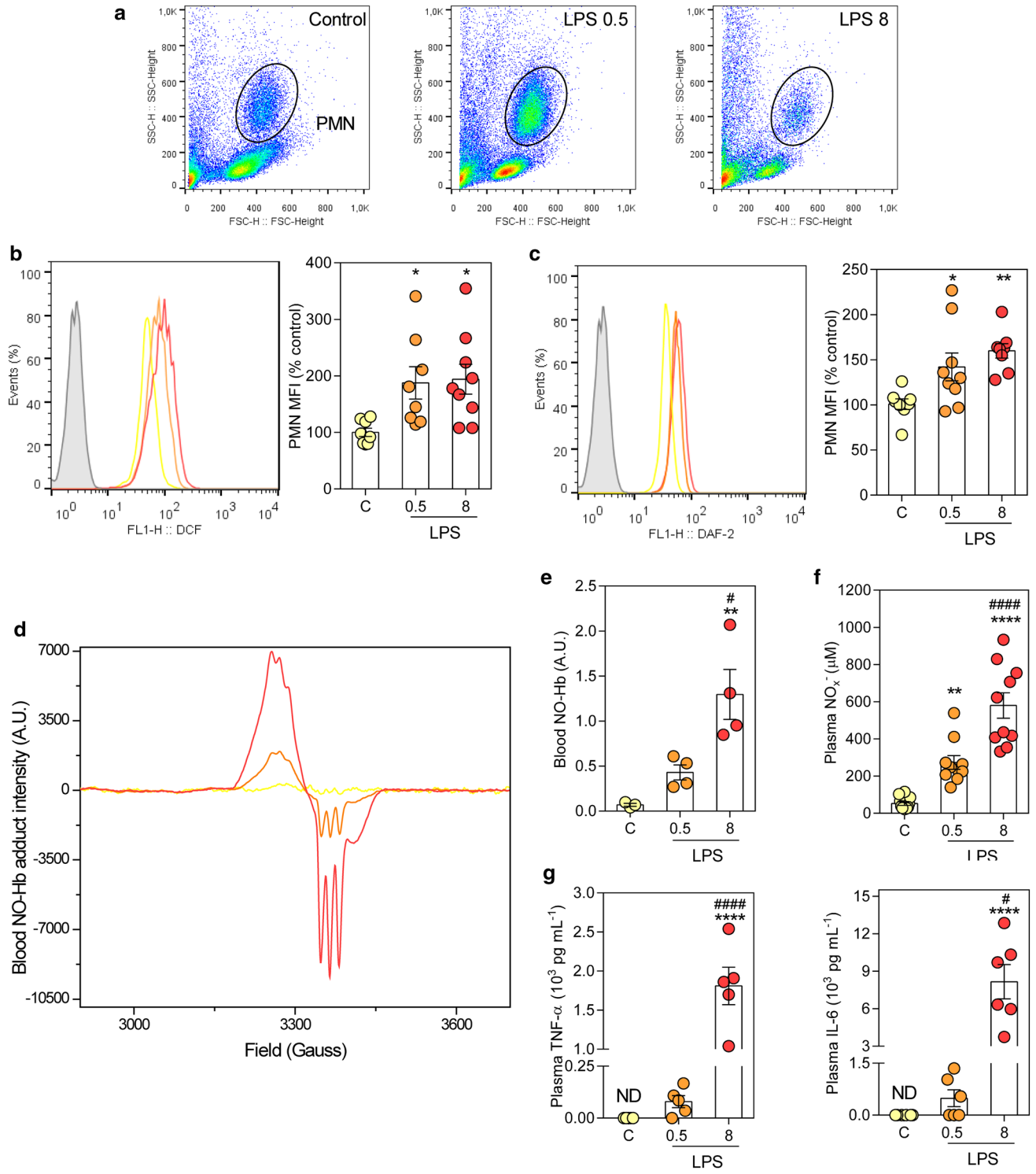

control animals ($p < 0.01$) in basal conditions (Fig. 2c). This effect was more evident when the relaxation response was analyzed after a β-adrenergic stimulus, expressed as Δt_{50}. While a 33% decrease was observed in control animals, Δt_{50} was − 24% in low-grade and − 14% in severe endotoxemia ($p < 0.05$), respectively, thus indicating an impairment of the lusitropic reserve in hearts of endotoxemic animals (Fig. 2d). Interestingly, in basal conditions, imbalances were observed in the mechanisms of relaxation despite maintaining a contractile state preserved in severe endotoxemia. This situation

◂**Fig. 1** Systemic innate immune response and its relation to the severity of the endotoxemia. **a** PMN respiratory burst and NO production by flow cytometry. PMN population was selected based on light scattering properties and 30,000 events within PMN gate were collected. **b** Overlaid histogram of gated (PMN) events versus DCF fluorescence intensity: control (yellow), low-grade endotoxemia (orange), severe endotoxemia (red); and quantification as mean fluorescence intensity (MFI) DCF% control. **c** Overlaid histogram of gated (PMN) events versus DAF-2 fluorescence; and quantification as MFI DAF-2% control in each treatment. $^{*}p<0.05$ and $^{**}p<0.01$ by ANOVA-Tukey's test ($n=9$). **d** Blood NO levels in low-grade and severe endotoxemia measured by blood NO-Hb spectra EPR ($g=2.033$). **e** NO-Hb signal quantification in control and LPS-treated animals, $^{**}p<0.01$ compared to control and $^{\#}p<0.05$ compared to low-grade endotoxemic animals by ANOVA-Tukey's test ($n=4$). **f** Plasma nitrite/nitrate (NO_x^-) levels in control and LPS-treated animals. $^{**}p<0.01$ and $^{****}p<0.0001$ compared to the control group, and $^{\#\#\#\#}p<0.0001$ compared to low-grade endotoxemic animals by ANOVA-Tukey's test ($n=10$). **g** Plasma TNF-α and IL-6 content in control and LPS-treated animals. $^{****}p<0.0001$ as compared to the control group, and $^{\#}p<0.05$ and $^{\#\#\#\#}p<0.0001$ as compared to low-grade endotoxemic animals by ANOVA-Tukey's test ($n=6$). *ND* not detected

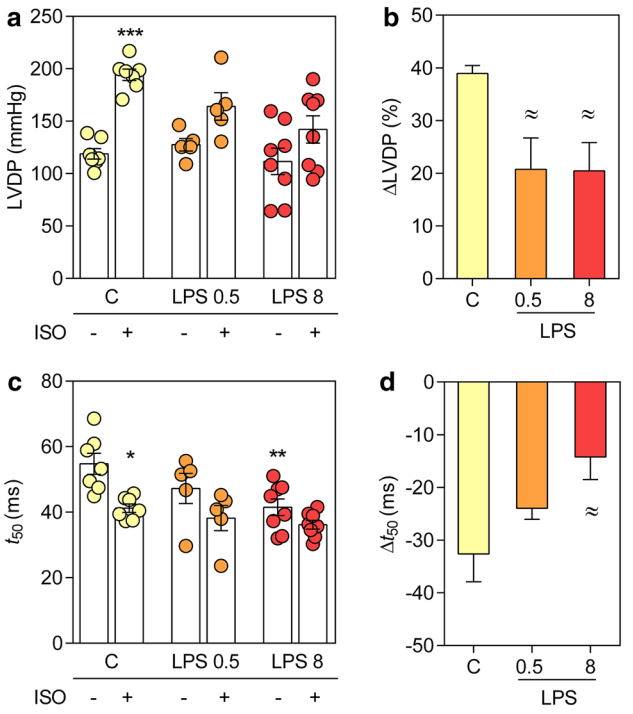

Fig. 2 Cardiac contractile and relaxation impairment in low-grade and severe endotoxemia. **a** Ventricular systolic function. Evaluation of left ventricular development pressure LVDP in basal conditions, and after a β-adrenergic stimulus with 1 μM ISO according to the Langendorff technique at constant flow; and **b** ventricular contractile reserve (ΔLVDP) calculated as the percentage increase in LVDP after ISO perfusion in each group. $^{***}p<0.001$ compared to the LVDP for the control group in basal conditions, $^{\approx}p<0.05$ compared to ΔLVDP in the control group by ANOVA-Tukey's test ($n=5$). **c** Ventricular diastolic function. Evaluation of isovolumic relaxation time (t_{50}) in basal conditions and after ISO according to the Langendorff technique at constant flow; and **d** ventricular lusitropic reserve (Δt_{50}) calculated as the percentage decrease in t_{50} after ISO perfusion in each group. $^{*}p<0.05$ and $^{**}p<0.01$ compared to t_{50} for control animals in basal conditions, $^{\approx}p<0.05$ compared to Δt_{50} in the control group by ANOVA-Tukey's test ($n=5$)

differed in the presence of work overload since both the contractile and relaxation mechanisms were found attenuated, even in low-grade inflammation.

Signs of inflammation were observed within cardiac tissue in both treated groups, being more evident in severe endotoxemia. Early phase pro-inflammatory cytokine mRNA transcripts, such as those for IL-1β and TNF-α, were found increased under both treatment conditions in the heart. As shown in Fig. 3a, mRNA transcripts for IL-1β increased in with LPS treatment, while mRNA transcripts for TNF-α were observed increased only in the severe endotoxemia group. Expression of IL-10 mRNA, an anti-inflammatory cytokine with regulatory functions, was assessed by endpoint PCR and was increased only in LPS 8 treatment (data not shown).

To study the possible causes of the cardiac dysfunction and inflammation, a histopathological analysis was performed. Myocardial tissue from control and LPS-treated animals exhibited a regular integrity of myocardial structure, normal cardiac muscle fibres, and no necrosis or leukocyte infiltration (Fig. 3b). However, different ultrastructural changes in myocardial tissue were evidenced in both LPS-treatments (Fig. 3c). Electron micrographs showed disorientation of myofibrils, disorder in inter-fibrillar mitochondria population (including different sizes of mitochondria), and interestingly, in sarcoplasmatic reticulum and mitochondrial junctions compared to control animals. These ultrastructural changes in cardiac tissue were even more evident in severe endotoxemia, where the loss of myofibrillar structure and abnormal mitochondria were also observed. Mitochondria swelling was observed with almost complete loss of the internal cristae structural pattern and loss of integrity of the inner membrane. Enlarged cytoplasmic vacuoles were also found in severe endotoxemic hearts (Fig. 3c).

Cardiac mitochondrial function is impaired with the severity of the endotoxemia

Mitochondrial function was studied by different approaches; mitochondrial respiration was analysed as the measurement of O_2 consumption in resting state (state 4), and in active state (state 3), which represents the maximal physiological rate of O_2 uptake and ATP synthesis. Although no statistical differences were observed for O_2 consumption in state 4 and state 3 between control and LPS-treated animals, a decrease in RCR in LPS-treated animals respect to control group was found ($p<0.05$) (Table 3). RCR is a sensitive indicator of mitochondrial integrity as its value depends on the degree

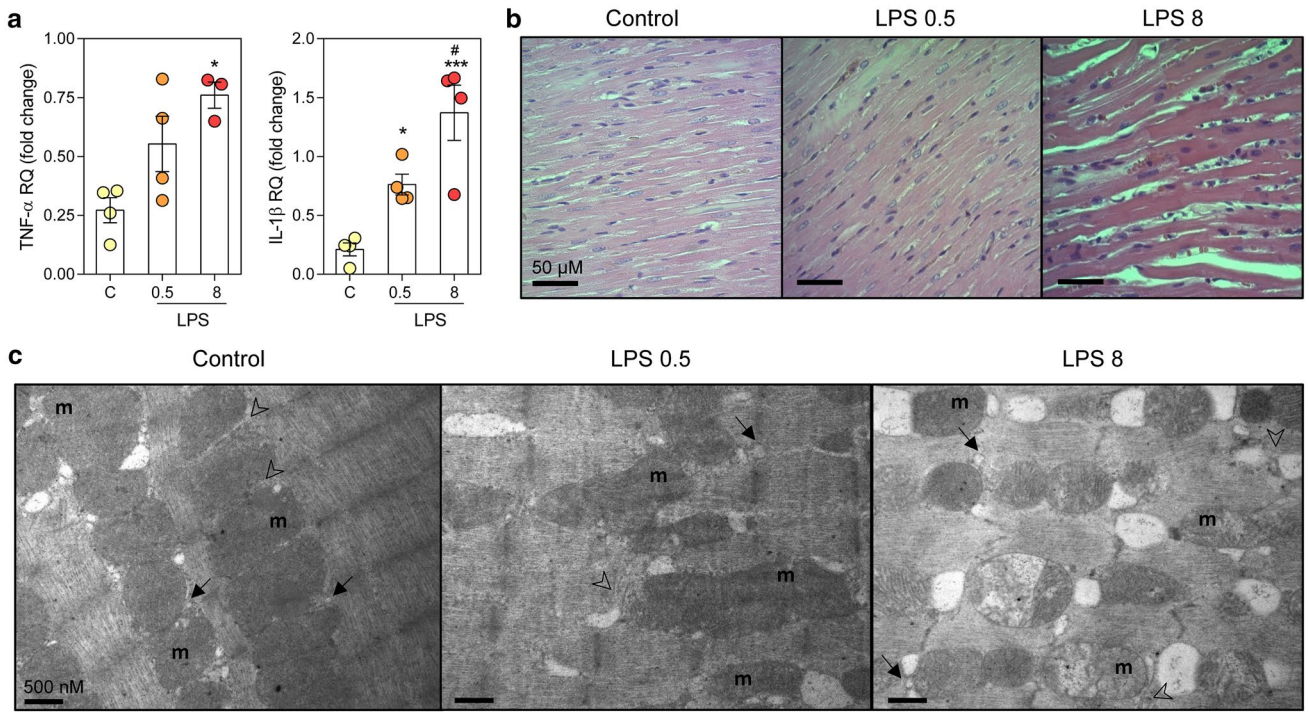

Fig. 3 Inflammatory sings in cardiac tissue, and changes in cardiac ultrastructure are evidenced during endotoxemia. **a** Relative quantification of mRNA transcripts for IL-1β and TNF-α assessed with respect to the β-actin mRNA, as housekeeping gene, by RT-qPCR. $^{*}p<0.05$ and $^{***}p<0.001$ compared to control group, and $^{\#}p<0.05$ compared to low-grade endotoxemic animals by ANOVA-Tukey's test ($n=4$). **b** Haematoxylin–eosin staining of cardiac tissue of control, low-grade, and severe endotoxemic animals. Magnification ×400. **c** Representative electron micrographs of cardiac myocyte sections comparing control and LPS-treated animals. Right: Control hearts showed normal myofibrillar morphology, with normal intra-fibrillar mitochondria (m), linked to sarcoplasmatic reticulum (arrowheads) and T-tubules (arrows). Middle: Heart from low-grade endotoxemia animals showed myofibrillar disarray. Left: Severe endotoxemia induced disarrangement of myofibrils and mitochondrial swelling and cristae disruption. Magnification ×20,000

of mitochondrial coupling, thus the decrease observed in RCR for low-grade and severe endotoxemia may indicate mitochondrial dysfunction. To deeply characterize this observation, ATP production rate was also evaluated, and a 30% decrease in the severe endotoxemia group was observed ($p<0.05$) (Fig. 4a). The number of phosphorylated ADP molecules per O_2 atom, calculated as P/O ratio, showed a tendency to decrease with the LPS dose (Fig. 4b). This may indicate that the efficiency of the oxidative phosphorylation process is impaired in both LPS treatments. Mitochondrial membrane potential was measured by flow cytometry, and a 13% decrease for low-grade endotoxemic animals ($p<0.05$) and a 20% decrease in severe endotoxemic animals ($p<0.01$) were observed compared to control animals (Fig. 4c–e). These results indicate the occurrence of mitochondrial inner membrane depolarization in both LPS treatments and agree with the observed alteration of mitochondrial oxidative phosphorylation. Due to the observation of altered mitochondrial bioenergetics, the activity of respiratory complexes was measured. As shown in Fig. 4f i, complex I–III activity decreased by 22% in the severe endotoxemia group compared to the control group ($p<0.05$). No significant differences were observed in complex II–III and complex IV activities (Fig. 4f ii–iii).

Table 3 Cardiac mitochondrial O_2 consumption impairment in endotoxemia

Mitochondrial O_2 consumption (malate + glutamate) (ng-at O min^{-1} mg $protein^{-1}$)			
	State 4	State 3	RCR[A]
Control	12.8 ± 1.1	75.3 ± 3.8	6.0 ± 0.3
Low-grade endotoxemia	15.2 ± 1.0	74.2 ± 3.8	5.0 ± 0.2*
Severe endotoxemia	15.0 ± 1.5	70.1 ± 4.9	4.8 ± 0.3*

$^{*}p<0.05$ as compared to control group by ANOVA-Tukey's test ($n=6$)

[A]Respiratory control ratio (RCR) was calculated as state 3/state 4 respiration rate

Cardiac mitochondrial dysfunction is related to oxidative and nitrosative stress

Both O_2^- and H_2O_2 are mainly produced in mitochondria. Depending on their steady-state concentrations, they can act as signaling molecules [44] or as mitochondrial macromolecule damaging oxidants [45]. Consequently, cardiac mitochondrial H_2O_2 production rate was measured and found increased by 40% ($p < 0.05$) in the low-grade endotoxemia group, and by 59% ($p < 0.01$) in the severe endotoxemia group, respect to control animals (Fig. 4g). These findings suggest that oxidative stress may be occurring in both LPS-treatments, and that may lead to mitochondrial dysfunction. As NO and H_2O_2 are increased in endotoxemia, nitrosative damage was evaluated as protein tyrosine nitration in isolated mitochondria (Fig. 4h, i). An increase in mitochondrial tyrosine nitration of about 66% for low-grade endotoxemia, and 82% for severe endotoxemia ($p < 0.05$) was observed, suggesting an increase in the steady-state concentration of $ONOO^-$. Moreover, a significant increase in nitrite/nitrate levels was observed in cardiac tissue for both endotoxemic groups (control: 3.5 ± 0.5, LPS 0.5: 7.8 ± 1.1, LPS 8: 8.5 ± 1 NO_x^- mg protein^{-1}, $p < 0.05$). These results are related to the increase in oxidative damage, supporting the hypothesis that oxidative and nitrosative stress are closely related mechanisms involved in the observed mitochondrial dysfunction in endotoxemia.

In vivo modulation of NO bioavailability partially restores cardiac and mitochondrial function

To elucidate if systemic NO levels determine mitochondrial and cardiac dysfunction in endotoxemia, an inhibitor of nitric oxide synthase (L-NAME) and a scavenger of blood NO (c-PTIO) were used in vivo to decrease systemic NO levels.

Co-treatment with L-NAME decreased blood NO-Hb levels in both endotoxemic groups (Fig. 5a i). Moreover, these results were confirmed by plasma NO_x^- content, which also showed a significant decrease in low-grade and severe endotoxemia animals compared with animals treated only with LPS ($p < 0.001$, Fig. 5a ii). As shown in Fig. 5a iii–iv, plasma TNF-α concentration was not altered with L-NAME co-treatment, although IL-6 levels in severe endotoxemia treated with L-NAME were found slightly increased ($p < 0.05$). This cytokine profile showed that the innate immune system remained activated despite L-NAME co-treatment; being this effect of L-NAME in agreement with previous observations [46, 47]. To analyze NO participation in cardiac function during endotoxemia, contractile state and cardiac relaxation were measured in animals treated with LPS plus L-NAME. As previously observed in endotoxemia, LVDP was not altered among the different experimental groups in basal conditions (Fig. 5b i). L-NAME treatment prevented the decrease in cardiac contractile reserve in low-grade and severe endotoxemia, resembling cardiac contractile reserve value in the control group (39% of %ΔLVDP) (Fig. 5b ii). Regarding relaxation time, L-NAME co-treatment during severe endotoxemia prevented relaxation response decay as t_{50} showed no statistical differences with the control group (Fig. 5b iii). This effect was also observed in the preservation of lusitropic reserve (expressed as $\%\Delta t_{50}$) of the severe endotoxemia group treated with L-NAME (Fig. 5b iv). Finally, to assess mitochondrial bioenergetics, inner membrane potential and ATP production rate were measured. As shown in Fig. 5c i, mitochondrial inner membrane remained unchanged with L-NAME co-treatment in low-grade and severe endotoxemia. Interestingly, mitochondrial ATP production rate increased with L-NAME co-treatment in severe endotoxemia ($p < 0.001$; Fig. 5c ii).

The administration of c-PTIO decreased systemic NO levels, measured as NO-Hb adduct (Fig. 6a i), where a 40% and 34% decrease was observed in the group of severe and low-grade endotoxemia with c-PTIO compared to the group treated only with LPS, respectively ($p < 0.05$). Plasma NO_x^- content was not affected by administration of c-PTIO (Fig. 6a ii), as expected and taking into account the mechanism of action of c-PTIO [48]. Plasma pro-inflammatory cytokine profile showed no alterations with the c-PTIO treatment compared with endotoxemia (Fig. 6a iii, iv). Regarding cardiac function, the differences observed with c-PTIO infusion were less evident than with L-NAME co-treatment. In this sense, a tendency to restore contractile and lusitropic reserve was observed (Fig. 6b). Mitochondrial bioenergetics was modulated by c-PTIO infusion. Mitochondrial inner membrane potential showed no difference between control and LPS plus c-PTIO treatment (Fig. 6c i). Moreover, ATP production rate was found increased when compared LPS 8 and LPS 8 + c-PTIO ($p < 0.05$) (Fig. 6c ii).

Discussion

In this work, the relationship between low-grade and severe endotoxemia with the systemic immune response, cardiac function, and mitochondrial performance is unravelled. Different previous studies have shown an association between cardiac function and NO levels [49], mitochondrial function and NO levels [50], and cardiac function and mitochondrial function [51]. To our knowledge, no studies have unravelled how NO levels and cytokine production, mitochondrial performance and cardiac contractile state are interconnected in the same animal model. The highlight of our experimental design was the study of two different LPS doses to

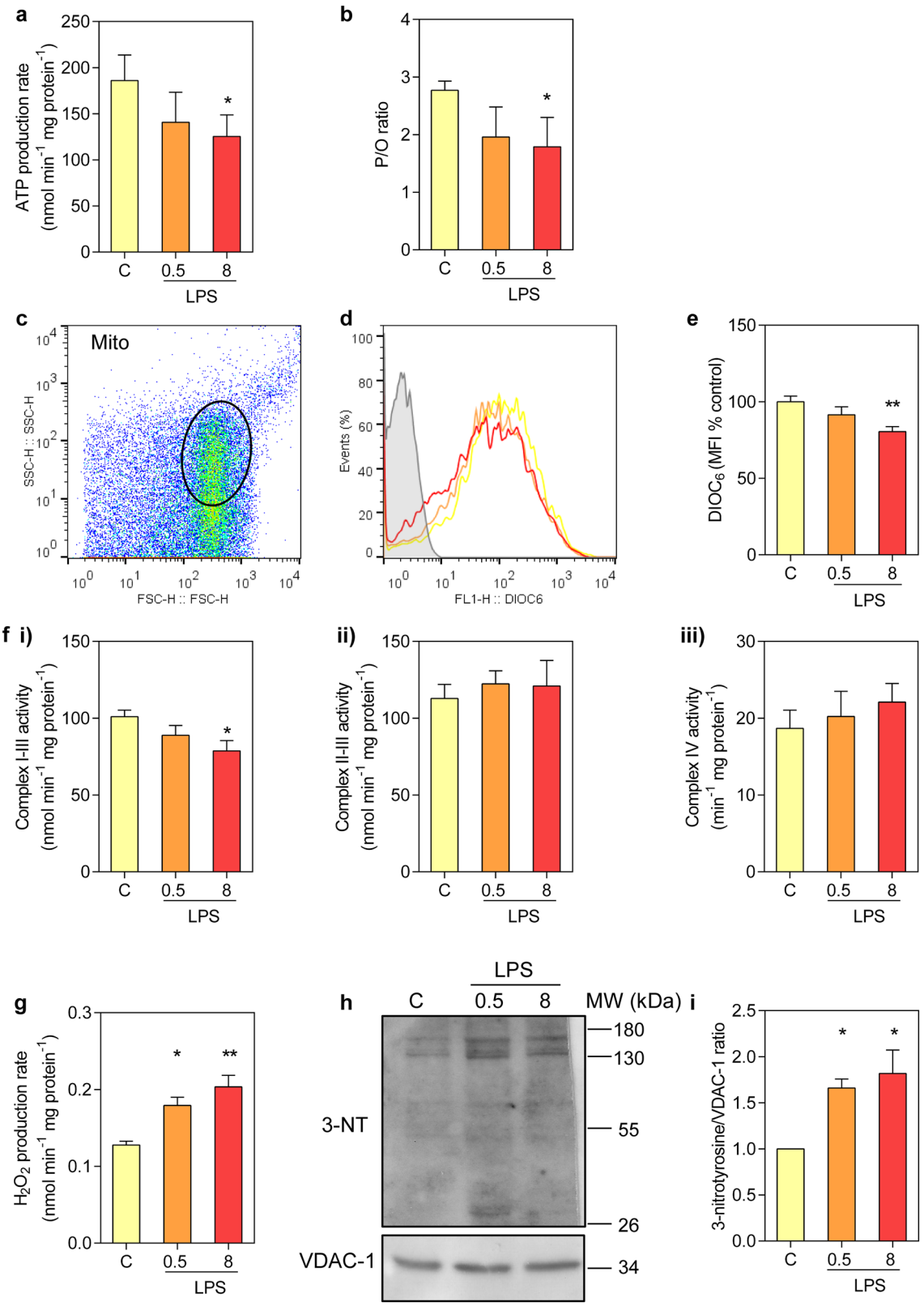
a
ATP production rate (nmol min-1 mg protein-1)
250
200
150
100
50
0
C
0.5
8
LPS
*
b
P/O ratio
4
3
2
1
0
C
0.5
8
LPS
*
c
Mito
SSC-H :: SSC-H
FSC-H :: FSC-H
d
Events (%)
FL1-H :: DIOC6
e
DIOC6 (MFI % control)
150
100
50
0
C
0.5
8
LPS
**
f i)
Complex I-III activity (nmol min-1 mg protein-1)
ii)
Complex II-III activity (nmol min-1 mg protein-1)
iii)
Complex IV activity (min-1 mg protein-1)
30
20
10
g
H2O2 production rate (nmol min-1 mg protein-1)
0.3
0.2
0.1
0.0
**
h
LPS
C
0.5
8
MW (kDa)
180
130
55
26
34
3-NT
VDAC-1
i
3-nitrotyrosine/VDAC-1 ratio
2.5
2.0
1.5
1.0
0.5
0.0

◂**Fig. 4** Cardiac mitochondrial dysfunction and oxidative and nitrosative stress in low grade and severe endotoxemia. **a** ATP production rate by isolated cardiac mitochondria using malate and glutamate as substrates, and **b** P/O ratio as the number of phosphorylated ADP molecules per O_2 atom consumed during active respiration, calculated for control and LPS-treated animals. $*p<0.05$ as compared to control group by ANOVA-Dunnett's test ($n=4$). **c** Cardiac mitochondrial inner membrane potential evaluated by flow cytometry. Representative dot plot of the samples: mitochondria population was selected based on light scattering properties and 30,000 events within Mito gate were collected. **d** Overlaid histograms of gated (Mito) mitochondrial events versus $DiOC_6$ fluorescence intensity. Control (yellow), low-grade endotoxemia group (orange), and severe endotoxemia group (red). **e** $DiOC_6$ fluorescence quantification as % control of gated (Mito) histogram, indicating cardiac mitochondrial inner membrane potential. $**p<0.01$ as compared to the control group by ANOVA-Tukey's test ($n=6$). **f** Cardiac mitochondrial respiratory chain complexes activities in control and LPS-treated animals: (i) complex I, (ii) complex II and (iii) complex IV activities. $*p<0.05$ as compared to control group by ANOVA-Dunnett's test ($n=7$). **g** H_2O_2 production rate by isolated cardiac mitochondria in the presence of malate and glutamate as substrates. $*p<0.05$ and $**p<0.01$ as compared to the control group by ANOVA-Tuckey's test ($n=6$). **h** Western blot analysis of isolated cardiac mitochondria using anti-3-nitrotyrosine antibody (upper panel) and anti-VDAC-1 antibody (lower panel) as loading control. (i) Densitometric unit ratio between 3-nitrotyrosine and VDAC-1. $*p<0.05$ as compared to control group by ANOVA-Tuckey's test ($n=3$)

generate two different inflammatory degrees, and the in vivo use of L-NAME or c-PTIO to modulate NO bioavailability, strengthening our conclusion.

Both experimental groups generated a typical acute systemic response given by the stimulation of the LPS. However, differences were observed in the systemic innate immune response between LPS doses. A marked decrease in the total leukocyte count in severe endotoxemia, and an increase in NO and proinflammatory cytokines in the circulation according to the severity of the inflammatory insult were found. As an increase in the percentage of neutrophils was observed, PMN activation was evaluated; increased ROS and NO production was found in both LPS treatments, supporting the activation of the cellular innate immune response in this model. NO is a key mediator in the inflammatory response in this type of syndrome, and it has been suggested to play an important role in most of the effects of inflammation: vasodilation, altered vascular permeability and extravasation, migration and activation of leucocytes [52]. In inflammatory situations, PMN and endothelial cells have been described as sources for increased NO production [53, 54]. Although its role in inflammation has not been described yet, is important to note that erythrocytes contain a functional eNOS, and may have a putative role in heart failure and atherosclerosis [55–57]. Since NO production by PMN was found increased, total NO levels in the bloodstream were measured for both LPS doses. A fivefold increase in low-grade endotoxemia animals and a 18-fold increase in severe endotoxemia animals were observed, indicating that there is an increase of NO generation from other sources apart from PMN production, which is different in both LPS treatments. These results agree with the view that the increase in the inflammatory response is closely related to the severity of endotoxemia. In this way, NO has a crucial role in the development of the inflammatory scenario, possibly leading to cardiac dysfunction.

Myocardial depression is a well-recognized manifestation of organ dysfunction in sepsis [58]. In the present study, we used the Langendorff technique to study myocardial function. Although this technique might is limited as it requires an isolated perfused heart, in our experimental setup, allowed us to independently study ventricular function from different variables such as load conditions, heart rate, circulating catecholamines, and pH [59, 60], that could modify the behavior of the global cardiac function apart from changes in mitochondrial function due to the inflammatory response. In our work, differences in isovolumetric relaxation time were observed in severe endotoxemia animals compared to control animals in basal conditions. It has been described that several pathophysiological entities develop diastolic dysfunction, with a contractile state remaining within normal parameters [61]. This result agrees with the higher amount of pro-inflammatory cytokines and NO in blood in these treated animals. Fernandes et al. described that, even at low doses, TNF-α and IL-1β are able to depress myocardial function in different biological systems, such as cardiomyocytes, animal models, and humans [11]. Additionally, NO has been described as a myocardial depressor [9, 12]. In this sense, our results showed that the in vivo modulation of NO by L-NAME and c-PTIO treatment partially prevented cardiac dysfunction. As this recovery was not complete, we cannot rule out the existence of alternative intrinsic mechanisms in the myocardium leading to altered contractile state when energy requirements rise in endotoxemia. For example, it has been reviewed by Kakihana, that β-adrenergic pathways are impaired in septic patients, and in experimental septic animals [12].

Cytokines production in the cardiac tissue could be involved as a depressor mechanism. It was described that cardiomyocytes can have an active role in inflammatory responses and release pro-inflammatory mediators in appropriate situations [62]. In the present work, both TNF-α and IL1-β were highly expressed in heart tissue, and these increases were related to the LPS dose. Moreover, the expression of anti-inflammatory cytokine IL-10 was only observed in severe endotoxemia animals, indicating that the compensatory regulation phase is activated, although not improving the resolution of the inflammatory scenario. Such observation suggests that cardiomyocytes can locally release factors that may ultimately damage the heart. It is worth noting that the ultrastructure of the severe endotoxemic myocardium showed fragmentation, disorientation and dissolution

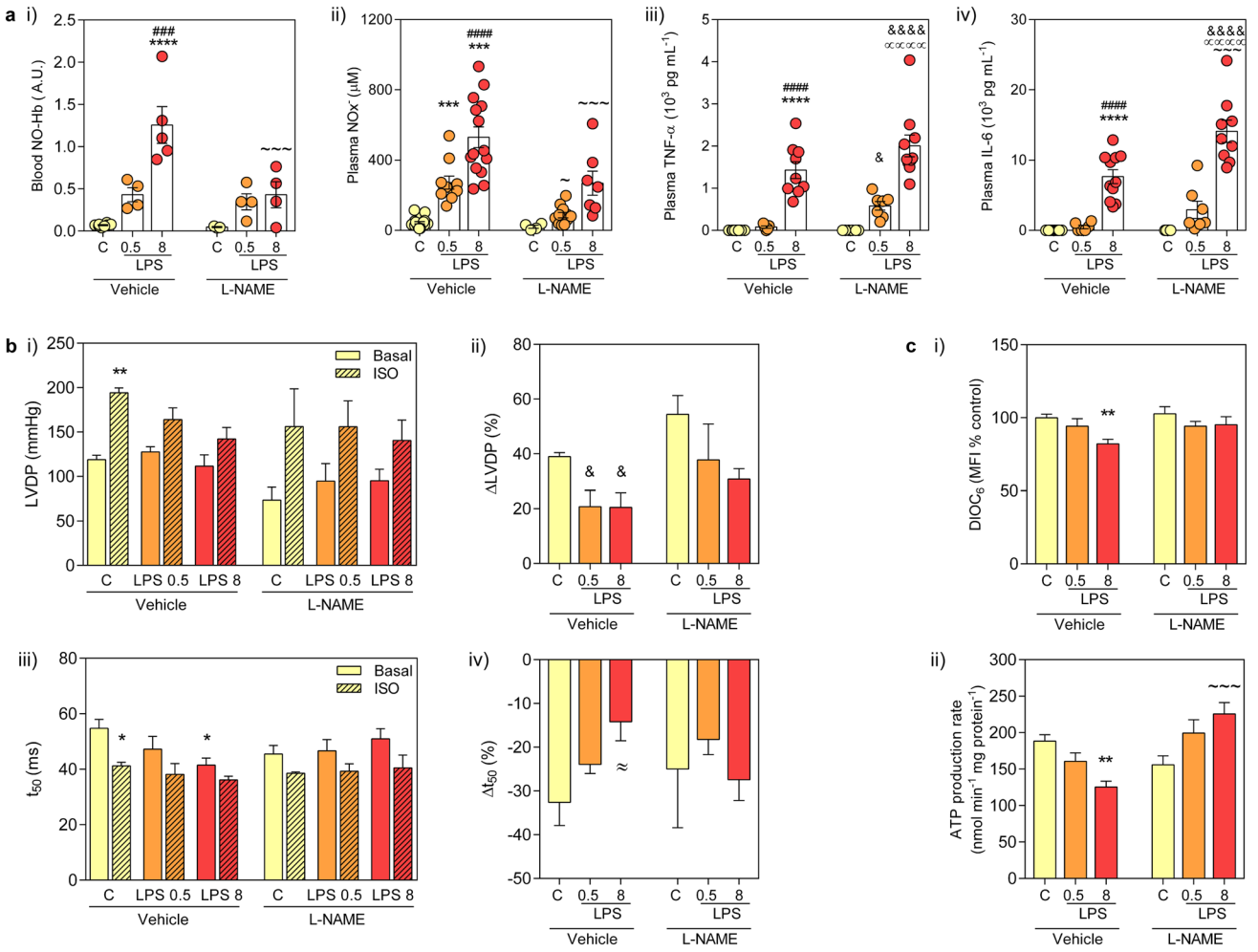

Fig. 5 Co-treatment with NOS synthase inhibitor, L-NAME, improves cardiac and mitochondrial function during endotoxemia. **a** *Evaluation of systemic innate immune response:* (i) NO determination in blood as NO-Hb adduct by EPR in LPS-treated animals co-injected with L-NAME. $^{****}p<0.0001$ compared to control group, $^{\#\#\#}p<0.001$ compared to LPS 0.5 animals, $^{\sim}p<0.05$ compared to LPS 0.5 animals, and $^{\sim\sim\sim}p<0.001$ compared to LPS 8 animals by ANOVA-Tukey's test ($n=4$). (ii) Plasma nitrite/nitrate (NO_x^-) levels in control and LPS-treated animals co-injected with L-NAME. $^{***}p<0.001$ compared to control group, $^{\#\#\#\#}p<0.0001$ compared to LPS 0.5 animals, and $^{\sim\sim\sim}p<0.001$ compared to LPS 8 animals by ANOVA-Tukey's test ($n=7$). (iii) Plasma TNF-α and (iv) IL-6 content in control and LPS-treated animals, co-treated with L-NAME. $^{****}p<0.0001$ as compared to control group, $^{\#\#\#\#}p<0.0001$ as compared to LPS 0.5 group, $^{\&}p<0.05$ and $^{\&\&\&\&}p<0.0001$ compared to L-NAME group, $^{\alpha\alpha\alpha\alpha}p<0.0001$ compared to LPS 0.5+L-NAME group, and $^{\sim\sim\sim}p<0.001$ compared to LPS 8 group by ANOVA-Tukey's test ($n=9$). **b** *Ventricular systolic and diastolic function*: (i) measurement of LVDP in basal conditions, and after a β-adrenergic stimulus with 1 μM ISO; and (ii) ventricular contractile reserve (ΔLVDP) calculated as the percentage increase in LVDP after ISO perfusion in each group. $^{**}p<0.01$ compared to the corresponding LVDP in basal conditions, $^{\&}p<0.05$ compared to ΔLVDP of L-NAME group by ANOVA-Tukey's test ($n=4$). (iii) Evaluation of isovolumic relaxation time (t_{50}) in basal conditions and after ISO; and (iv) ventricular lusitropic reserve (Δt_{50}) calculated as the percentage decrease in t_{50} after ISO perfusion in each group. $^{*}p<0.05$ compared to t_{50} in control group in basal conditions, $^{\approx}p<0.05$ compared to Δt_{50} in the control group by ANOVA-Tukey's test ($n=4$). **c** *Cardiac mitochondrial function*: (i) cardiac mitochondrial inner membrane potential evaluated by flow cytometry using $DiOC_6$ probe. $^{**}p<0.01$ as compared to control group by ANOVA-Tukey's test ($n=5$). (ii) Cardiac mitochondrial ATP production rate. $^{**}p<0.01$ as compared to control group, and $^{\sim\sim\sim}p<0.001$ compared to LPS 8 group by ANOVA-Tukey's test ($n=5$)

of myofibrils, and an increase in the t-tubules spaces, which leads a disruption in sarcoplasmatic reticulum and mitochondria junction. This observation agrees with the cardiac function impairment observed in severe endotoxemia. Some of these changes were also observed in low-grade endotoxemia, where only a partial loss of myofibril order and a loss of pattern of mitochondrial and sarcoplasmatic reticulum junction were found. Therefore, the impairment of the contractile elements and the relationship with these depressant molecules should continue under study in these inflammatory syndromes.

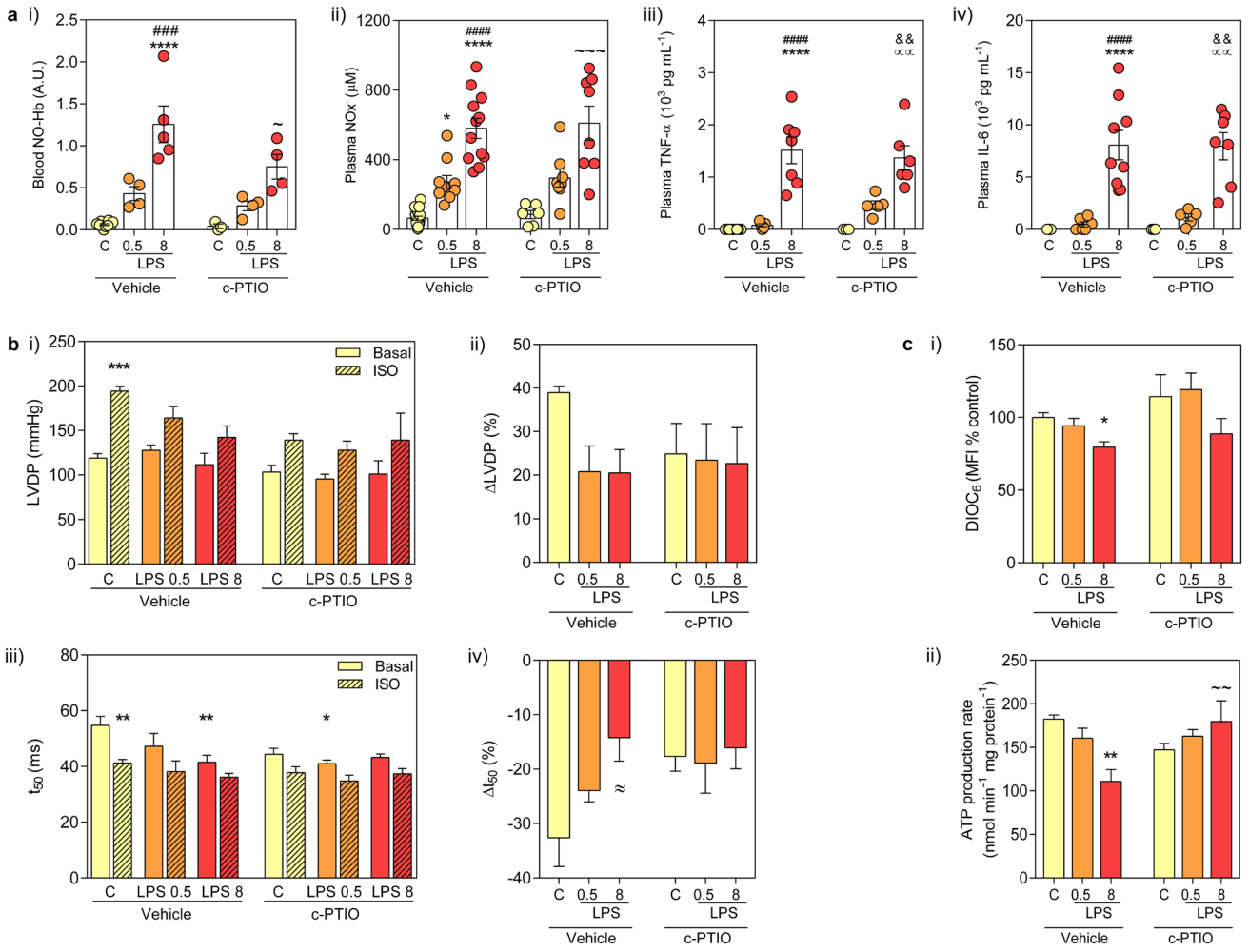

Fig. 6 Administration of the NO scavenger, c-PTIO, improves mitochondrial function during endotoxemia. **a** *Evaluation of systemic innate immune response*: (i) NO determination in blood as NO-Hb adduct by EPR in low-grade and severe endotoxemia with c-PTIO administration. $^{****}p<0.0001$ compared to control animals, $^{\#\#\#}p<0.001$ compared to LPS 0.5 animals, and $^{\sim}p<0.05$ compared to LPS 8 animals by ANOVA-Tukey's test ($n=4$). (ii) Plasma nitrite/nitrate (NO_x^-) levels in control and LPS-treated animals with c-PTIO administration. $^{*}p<0.05$ and $^{****}p<0.0001$ compared to control animals, $^{\#\#\#\#}p<0.0001$ compared to LPS 0.5 animals, and $^{\sim\sim\sim}p<0.001$ compared to LPS 8 animals by ANOVA-Tukey's test ($n=8$). (iii) Plasma TNF-α and (iv) IL-6 content in control and LPS-treated animals with c-PTIO administration. $^{****}p<0.0001$ as compared to control group, $^{\#\#\#\#}p<0.0001$ as compared to LPS 0.5 group, $^{\&\&}p<0.01$ as compared to c-PTIO group, $^{\propto\propto}p<0.01$ compared to LPS 0.5 + c-PTIO group by ANOVA-Tukey's test ($n=6$). **b** *Ventricular systolic and diastolic function*: (i) evaluation of LVDP in basal conditions, and after a β-adrenergic stimulus with 1 μM ISO; and (ii) ventricular contractile reserve (ΔLVDP) calculated as the percentage increase in LVDP after ISO perfusion in each group. $^{***}p<0.001$ compared to the corresponding LVDP in basal conditions by ANOVA-Tukey's test ($n=4$). (iii) Evaluation of isovolumic relaxation time (t_{50}) in basal conditions and after ISO; and (iv) ventricular lusitropic reserve (Δt_{50}) calculated as the percentage decrease in t_{50} after ISO perfusion in each group. $^{*}p<0.05$ and $^{**}p<0.01$ compared to t_{50} in control group in basal conditions; $^{\approx}p<0.05$ compared to Δt_{50} in the control group by ANOVA-Tukey's test ($n=4$). (c) *Cardiac mitochondrial function*: (i) cardiac mitochondrial inner membrane potential evaluated by flow cytometry using $DiOC_6$ probe. $^{*}p<0.05$ as compared to control group by ANOVA-Tukey's test ($n=4$). (ii) Cardiac mitochondrial ATP production rate. $^{**}p<0.01$ as compared to the control group, and $^{\sim\sim}p<0.01$ compared to LPS 8 group by ANOVA-Tukey's test ($n=4$)

The heart requires large amounts of energy to sustain contractile function and is the major consumer of energy in the body on a weight basis. Patients who died from sepsis showed myocarditis, disruption of the contractile apparatus, increased amounts of interstitial collagen, and damaged mitochondria [20]. Brealey et al. suggested that ATP content may be related to patient outcome [13]. In line with these findings, we observed that mitochondrial function is impaired as the severity of the endotoxemia increases. Mitochondrial dysfunction was characterized by decreased mitochondrial O_2 consumption, mitochondrial inner membrane potential, and ATP production in severe endotoxemia. Mitochondrial efficiency, estimated by P/O ratio, was found decreased in severe endotoxemia. The whole scenario

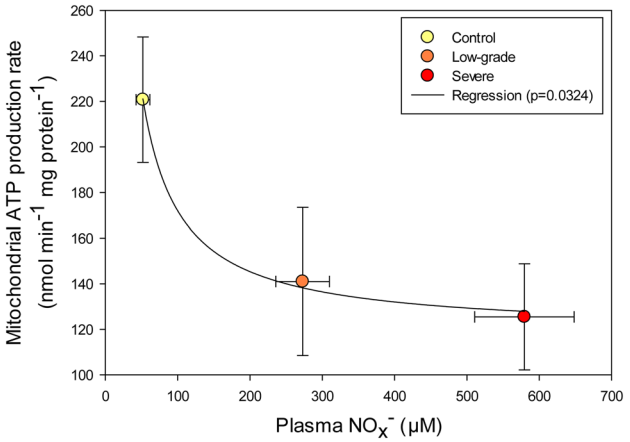

Fig. 7 Nitrite/nitrate levels in blood correlate with the decrease in cardiac mitochondrial ATP production rate

consequently leads to decreased ATP availability. Interestingly, the difference between resting and active mitochondrial respiration is known as mitochondrial reserve capacity; this reserve allows cardiomyocytes to properly respond to enhanced energetic demand [63]. The values calculated (63, 59 and 55 ng at O min^{-1} mg $protein^{-1}$ for control, low-grade, and severe endotoxemia, respectively) from Table 3, agree with the cardiac compromise observed only after a β-adrenergic stimulus. This analysis demonstrates that mitochondrial bioenergetics is of importance in the cardiac contractility status.

We have previously shown that mitochondrial ROS and NO production in different tissues contribute to mitochondrial dysfunction in endotoxemia [40, 64]. In the present work, analyzing different endotoxemia grades, we found a hyperbolic correlation of nitrite/nitrate levels in plasma with cardiac mitochondrial ATP production rate (Fig. 7), indicating the key and complex role of NO in modulating the mitochondrial respiratory chain. At low concentrations, it acts as a competitive inhibitor with O_2 in complex IV active site reversibly inhibiting oxidative phosphorylation; while in similar or higher concentrations, and in the presence of O_2^-, $ONOO^-$ is produced and it irreversibly inhibits complex I and III [17, 65, 66]. A positive correlation was observed in this experimental model between the decrease in mitochondrial function and the increase in cardiac mitochondrial H_2O_2 production, NO and $ONOO^-$ levels. Inhibition of complex I was observed at the highest concentration of NO in severe endotoxemia, associated with decreased mitochondrial inner membrane potential, decreased mitochondrial respiratory control ratio, thus yielding diminished ATP production. Moreover, the fact that low-grade endotoxemia only showed partial mitochondrial dysfunction, may indicate that cardiac bioenergetics is started to be affected even at a low-grade inflammatory stimulus, being this observation important during the progression of other inflammatory human conditions such as metabolic endotoxemia [7]. Ultrastructural changes in myofibrils and mitochondria population emerge as an interesting field to be analysed in low-grade inflammation.

Interestingly, in vivo modulation of blood NO levels with L-NAME and c-PTIO partially prevented the observed mitochondrial and cardiac dysfunction in endotoxemia. Moreover, the improvement observed occurred independently from systemic pro-inflammatory response. In this sense, the key implication of our study is that the inflammatory insult mainly determined by NO blood levels has a causal relationship with decreased mitochondrial bioenergetics and ultimately cardiac contractile state. Further studies are needed to elucidate other mitochondrial pathways related to cell and organ dysfunction in the heart. Unravelling the mechanisms involved in the onset of sepsis and endotoxemia would improve not only the interpretation of the pathology but also would provide new possibilities for the generation of novel therapeutic targets for treatment in the clinic as well.

Acknowledgements The authors are grateful to Daniel Gonzalez Maglio for the helpful assistance with ELISA assays, to Elizabeth Robello for the assistance with EPR assays, and to Pablo La Padula for his helpful analysis of cardiac function.

Funding This work was supported by research Grants from the Secretaría de Ciencia y Técnica, University of Buenos Aires [UBACYT2016 20020150100186BA]; Agencia Nacional de Promoción Científica y Tecnológica (ANPCYT) [PICT 2013-3227]; and Consejo Nacional de Investigaciones Científicas y Técnicas (CONICET) [PIP 11220120100321].

Compliance with ethical standards

Conflict of interest The authors declare no conflict of interest.

References

1. Singer M, Deutschman CS, Seymour CW, Shankar-Hari M, Annane D, Bauer M, Bellomo R, Bernard GR, Chiche JD, Coopersmith CM, Hotchkiss RS, Levy MM, Marshall JC, Martin GS, Opal SM, Rubenfeld GD, van der Poll T, Vincent JL, Angus DC, Der Poll T, Vincent JL, Angus DC (2016) The third international consensus definitions for sepsis and septic shock (Sepsis-3). JAMA 315:801–810. https://doi.org/10.1001/jama.2016.0287
2. Cohen J, Vincent J-L, Adhikari NKJ, Machado FR, Angus DC, Calandra T, Jaton K, Giulieri S, Delaloye J, Opal S, Tracey K, van der Poll T, Pelfrene E (2015) Sepsis: a roadmap for future research. Lancet Infect Dis 15:581–614. https://doi.org/10.1016/S1473-3099(15)70112-X
3. Thimmulappa RK, Scollick C, Traore K, Yates M, Trush MA, Liby KT, Sporn MB, Yamamoto M, Kensler TW, Biswal S (2006) Nrf2-dependent protection from LPS induced inflammatory response and mortality by CDDO-Imidazolide. Biochem

Biophys Res Commun 351:883–889. https://doi.org/10.1016/j.bbrc.2006.10.102
4. Morris MC, Gilliam EA, Li L (2014) Innate immune programing by endotoxin and its pathological consequences. Front Immunol 5:680. https://doi.org/10.3389/fimmu.2014.00680
5. Cani PD, Amar J, Iglesias MA, Poggi M, Knauf C, Bastelica D, Neyrinck AM, Fava F, Tuohy KM, Chabo C, Waget A, Delmée E, Cousin B, Sulpice T, Chamontin B, Ferrières J, Tanti J-FF, Gibson GR, Casteilla L, Delzenne NM, Alessi MC, Burcelin R (2007) Metabolic endotoxemia initiates obesity and insulin resistance. Diabetes 56:1761–1772. https://doi.org/10.2337/db06-1491
6. Frisard MI, McMillan RP, Marchand J, Wahlberg KA, Wu Y, Voelker KA, Heilbronn L, Haynie K, Muoio B, Li L, Hulver MW (2010) Toll-like receptor 4 modulates skeletal muscle substrate metabolism. Am J Physiol Endocrinol Metab 298:E988–E998. https://doi.org/10.1152/ajpendo.00307.2009
7. Glaros TG, Chang S, Gilliam EA, Maitra U, Deng H, Li L (2013) Causes and consequences of low grade endotoxemia and inflammatory diseases. Front Biosci (Schol Ed) 5:754–765. https://doi.org/10.2741/s405
8. de Punder K, Pruimboom L (2015) Stress induces endotoxemia and low-grade inflammation by increasing barrier permeability. Front Immunol 6:223. https://doi.org/10.3389/fimmu.2015.00223
9. Antonucci E, Fiaccadori E, Donadello K, Taccone FS, Franchi F, Scolletta S (2014) Myocardial depression in sepsis: from pathogenesis to clinical manifestations and treatment. J Crit Care 29:500–511. https://doi.org/10.1016/j.jcrc.2014.03.028
10. Celes MR, Prado CM, Rossi MA (2013) Sepsis: going to the heart of the matter. Pathobiology 80:70–86. https://doi.org/10.1159/000341640
11. Fernandes CJ Jr, de Assuncao MS (2012) Myocardial dysfunction in sepsis: a large, unsolved puzzle. Crit Care Res Pr 2012:896430. https://doi.org/10.1155/2012/896430
12. Kakihana Y, Ito T, Nakahara M, Yamaguchi K, Yasuda T (2016) Sepsis-induced myocardial dysfunction: pathophysiology and management. J Intensive Care 4:22. https://doi.org/10.1186/s40560-016-0148-1
13. Brealey D, Brand M, Hargreaves I, Heales S, Land J, Smolenski R, Davies NA, Cooper CE, Singer M (2002) Association between mitochondrial dysfunction and severity and outcome of septic shock. Lancet 360:219–223. https://doi.org/10.1016/S0140-6736(02)09459-X
14. Carre JE, Orban JC, Re L, Felsmann K, Iffert W, Bauer M, Suliman HB, Piantadosi CA, Mayhew TM, Breen P, Stotz M, Singer M (2010) Survival in critical illness is associated with early activation of mitochondrial biogenesis. Am J Respir Crit Care Med 182:745–751. https://doi.org/10.1164/rccm.201003-0326OC
15. Fink MP (2001) Cytopathic hypoxia. Mitochondrial dysfunction as mechanism contributing to organ dysfunction in sepsis. Crit Care Clin 17:219–237. https://doi.org/10.1016/S0749-0704(05)70161-5
16. Flierl M, Rittirsch D, Huber-Lang MS, Sarma JV, Ward PA (2008) Molecular events in the cardiomyopathy of sepsis. Mol Med 14:1. https://doi.org/10.2119/2007-00130.Flierl
17. Radi R, Cassina A, Hodara R, Quijano C, Castro L (2002) Peroxynitrite reactions and formation in mitochondria. Free Radic Biol Med 33:1451–1464. https://doi.org/10.1016/S0891-5849(02)01111-5
18. Vanasco V, Saez T, Magnani ND, Pereyra L, Marchini T, Corach A, Vaccaro MI, Corach D, Evelson P, Alvarez S (2014) Cardiac mitochondrial biogenesis in endotoxemia is not accompanied by mitochondrial function recovery. Free Radic Biol Med 77:1–9. https://doi.org/10.1016/j.freeradbiomed.2014.08.009
19. Bøtker HE, Hausenloy D, Andreadou I, Antonucci S, Boengler K, Davidson SM, Deshwal S, Devaux Y, Di Lisa F, Di Sante M, Efentakis P, Femminò S, García-Dorado D, Giricz Z, Ibanez B, Iliodromitis E, Kaludercic N, Kleinbongard P, Neuhäuser M, Ovize M, Pagliaro P, Rahbek-Schmidt M, Ruiz-Meana M, Schlüter K-D, Schulz R, Skyschally A, Wilder C, Yellon DM, Ferdinandy P, Heusch G (2018) Practical guidelines for rigor and reproducibility in preclinical and clinical studies on cardioprotection. Basic Res Cardiol 113:39. https://doi.org/10.1007/s00395-018-0696-8
20. Alvarez S, Vico T, Vanasco V (2016) Cardiac dysfunction, mitochondrial architecture, energy production, and inflammatory pathways: interrelated aspects in endotoxemia and sepsis. Int J Biochem Cell Biol 81:307–314. https://doi.org/10.1016/j.biocel.2016.07.032
21. Yao Y, Hu X, Feng X, Zhao Y, Song M, Wang C, Fan H (2019) Dexmedetomidine alleviates lipopolysaccharide-induced acute kidney injury by inhibiting the NLRP3 inflammasome activation via regulating the TLR4/NOX4/NF-κB pathway. J Cell Biochem. https://doi.org/10.1002/jcb.29173
22. Natanson C, Eichenholz PW, Danner RL, Eichacker PQ, Hoffman WD, Kuo GC, Banks SM, MacVittie TJ, Parrillo JE (1989) Endotoxin and tumor necrosis factor challenges in dogs simulate the cardiovascular profile of human septic shock. J Exp Med 169:823–832. https://doi.org/10.1084/jem.169.3.823
23. Zhang H-X, Liu S-J, Tang X-L, Duan G-L, Ni X, Zhu X-Y, Liu Y-J, Wang C-N (2016) H2S attenuates LPS-induced acute lung injury by reducing oxidative/nitrative stress and inflammation. Cell Physiol Biochem 40:1603–1612. https://doi.org/10.1159/000453210
24. Miura K, Yamanaka S, Ebara T, Okumura M, Imanishi M, Kim S, Nakatani T, Iwao H (2000) Effects of nitric oxide scavenger, carboxy-PTIO on endotoxin-induced alterations in systemic hemodynamics in rats. Jpn J Pharmacol 82:261–264
25. Yoshida M, Akaike T, Wada Y, Sato K, Ikeda K, Ueda S, Maeda H (1994) Therapeutic effects of imidazolineoxyl N-oxide against endotoxin shock through its direct nitric oxide-scavenging activity. Biochem Biophys Res Commun 202:923–930. https://doi.org/10.1006/bbrc.1994.2018
26. Marchini T, Magnani ND, Paz ML, Vanasco V, Tasat D, Gonzalez Maglio DH, Alvarez S, Evelson PA (2014) Time course of systemic oxidative stress and inflammatory response induced by an acute exposure to residual oil fly ash. Toxicol Appl Pharmacol 274:274–282. https://doi.org/10.1016/j.taap.2013.11.013
27. Walrand S, Valeix S, Rodriguez C, Ligot P, Chassagne J, Vasson M-P (2003) Flow cytometry study of polymorphonuclear neutrophil oxidative burst: a comparison of three fluorescent probes. Clin Chim Acta 331:103–110. https://doi.org/10.1016/S0009-8981(03)00086-X
28. Miranda KM, Espey MG, Wink DA (2001) A rapid, simple spectrophotometric method for simultaneous detection of nitrate and nitrite. Nitric Oxide 5:62–71. https://doi.org/10.1006/niox.2000.0319
29. Buchholz B, D'Annunzio VV, Giani JF, Siachoque N, Dominici FP, Turyn D, Perez V, Donato MM, Gelpi RJ (2014) Ischemic postconditioning reduces infarct size through the alpha1-adrenergic receptor pathway. J Cardiovasc Pharmacol 63:504–511. https://doi.org/10.1097/fjc.0000000000000074
30. Sutherland FJ, Shattock MJ, Baker KE, Hearse DJ (2003) Mouse isolated perfused heart: characteristics and cautions. Clin Exp Pharmacol Physiol 30:867–878. https://doi.org/10.1046/j.1440-1681.2003.03925.x
31. Jain M, Lim CC, Nagata K, Davis VM, Milstone DS, Liao R, Mortensen RM (2001) Targeted inactivation of Galpha(i) does not alter cardiac function or beta-adrenergic sensitivity. Am J Physiol Hear Circ Physiol 280:H569–H575. https://doi.org/10.1152/ajpheart.2001.280.2.H569
32. Marchini T, D'Annunzio V, Paz ML, Cáceres L, Garcés M, Perez V, Tasat D, Vanasco V, Magnani N, Gonzalez Maglio

D, Gelpi RJ, Alvarez S, Evelson P (2015) Selective TNF-α targeting with infliximab attenuates impaired oxygen metabolism and contractile function induced by an acute exposure to air particulate matter. Am J Physiol Heart Circ Physiol 309:H1621–H1628. https://doi.org/10.1152/ajpheart.00359.2015
33. Mela L, Seitz S (1979) Isolation of mitochondria with emphasis on heart mitochondria from small amounts of tissue. Methods Enzym 55:39–46
34. Cadenas E, Boveris A (1980) Enhancement of hydrogen peroxide formation by protophores and ionophores in antimycin-supplemented mitochondria. Biochem J 188:31–37
35. Lowry OH, Rosebrough NJ, Farr AL, Randall RJ (1951) Protein measurement with the Folin phenol reagent. J Biol Chem 193:265–275. https://doi.org/10.1016/0304-3894(92)87011-4
36. Boveris A, Costa LE, Cadenas E, Poderoso JJ (1999) Regulation of mitochondrial respiration by adenosine diphosphate, oxygen, and nitric oxide. Methods Enzym 301:188–198
37. Vives-Bauza C, Yang L, Manfredi G (2007) Assay of mitochondrial ATP synthesis in animal cells and tissues. Methods Cell Biol 80:155–171. https://doi.org/10.1016/S0091-679X(06)80007-5
38. Marchini T, Magnani N, D'Annunzio V, Tasat D, Gelpi RJ, Alvarez S, Evelson P (2013) Impaired cardiac mitochondrial function and contractile reserve following an acute exposure to environmental particulate matter. Biochim Biophys Acta Gen Subj 1830:2545–2552. https://doi.org/10.1016/j.bbagen.2012.11.012
39. Haines TH, Dencher NA (2002) Cardiolipin: a proton trap for oxidative phosphorylation. FEBS Lett 528:35–39. https://doi.org/10.1016/S0014-5793(02)03292-1
40. Vanasco V, Magnani ND, Cimolai MC, Valdez LB, Evelson P, Boveris A, Alvarez S (2012) Endotoxemia impairs heart mitochondrial function by decreasing electron transfer, ATP synthesis and ATP content without affecting membrane potential. J Bioenerg Biomembr 44:243–252. https://doi.org/10.1007/s10863-012-9426-3
41. Yonetani T (1967) Cytochrome oxidase: beef heart. In: Methods in enzymology. pp 332–335. https://doi.org/10.1016/0076-6879(67)10062-1
42. Chen Q, Vazquez EJ, Moghaddas S, Hoppel CL, Lesnefsky EJ (2003) Production of reactive oxygen species by mitochondria: central role of complex III. J Biol Chem 278:36027–36031. https://doi.org/10.1074/jbc.m304854200
43. Bryan NS, Grisham MB (2007) Methods to detect nitric oxide and its metabolites in biological samples. Free Radic Biol Med 43:645–657. https://doi.org/10.1016/j.freeradbiomed.2007.04.026
44. Antunes F, Cadenas E (2001) Cellular titration of apoptosis with steady state concentrations of H_2O_2: submicromolar levels of H_2O_2 induce apoptosis through fenton chemistry independent of the cellular thiol state. Free Radic Biol Med 30:1008–1018. https://doi.org/10.1016/S0891-5849(01)00493-2
45. Vanasco V, Evelson P, Boveris A, Alvarez S (2010) In situ and real time muscle chemiluminescence determines singlet oxygen involvement in oxidative damage during endotoxemia. Chem Biol Interact 184:313–318. https://doi.org/10.1016/j.cbi.2010.01.011
46. Connelly L, Palacios-Callender M, Ameixa C, Moncada S, Hobbs AJ (2001) Biphasic regulation of NF-kappa B activity underlies the pro- and anti-inflammatory actions of nitric oxide. J Immunol 166:3873–3881. https://doi.org/10.4049/jimmunol.166.6.3873
47. Walley KR, McDonald TE, Higashimoto Y, Hayashi S (1999) Modulation of proinflammatory cytokines by nitric oxide in murine acute lung injury. Am J Respir Crit Care Med 160:698–704. https://doi.org/10.1164/ajrccm.160.2.9809081
48. Millar CGM, Thiemermann C (2002) Carboxy-PTIO, a scavenger of nitric oxide, selectively inhibits the increase in medullary perfusion and improves renal function in endotoxemia. Shock 18:64–68
49. van de Sandt AM, Windler R, Gödecke A, Ohlig J, Zander S, Reinartz M, Graf J, van Faassen EE, Rassaf T, Schrader J, Kelm M, Merx MW (2013) Endothelial NOS (NOS3) impairs myocardial function in developing sepsis. Basic Res Cardiol 108:330. https://doi.org/10.1007/s00395-013-0330-8
50. Ortiz F, García JA, Acuña-Castroviejo D, Doerrier C, López A, Venegas C, Volt H, Luna-Sánchez M, López LC, Escames G (2014) The beneficial effects of melatonin against heart mitochondrial impairment during sepsis: inhibition of iNOS and preservation of nNOS. J Pineal Res 56:71–81. https://doi.org/10.1111/jpi.12099
51. Jarkovska D, Markova M, Horak J, Nalos L, Benes J, Al-Obeidallah M, Tuma Z, Sviglerova J, Kuncova J, Matejovic M, Stengl M (2018) Cellular mechanisms of myocardial depression in porcine septic shock. Front Physiol 9:726. https://doi.org/10.3389/fphys.2018.00726
52. Kirkeboen KA, Strand OA (1999) The role of nitric oxide in sepsis—an overview. Acta Anaesthesiol Scand 43:275–288
53. Aird WC (2003) The role of the endothelium in severe sepsis and multiple organ dysfunction syndrome. Blood 101:3765–3777. https://doi.org/10.1182/blood-2002-06-1887
54. Predonzani A, Cali B, Agnellini AH, Molon B, Calì B, Agnellini AH, Molon B, Cali B, Agnellini AH, Molon B (2015) Spotlights on immunological effects of reactive nitrogen species: when inflammation says nitric oxide. World J Exp Med 5:64–76. https://doi.org/10.5493/wjem.v5.i2.64
55. Cortese-Krott MM, Rodriguez-Mateos A, Sansone R, Kuhnle GGC, Thasian-Sivarajah S, Krenz T, Horn P, Krisp C, Wolters D, Heiß C, Kröncke K-D, Hogg N, Feelisch M, Kelm M (2012) Human red blood cells at work: identification and visualization of erythrocytic eNOS activity in health and disease. Blood 120:4229–4237. https://doi.org/10.1182/blood-2012-07-442277
56. Kleinbongard P, Schulz R, Rassaf T, Lauer T, Dejam A, Jax T, Kumara I, Gharini P, Kabanova S, Ozüyaman B, Schnürch H-G, Gödecke A, Weber A-A, Robenek M, Robenek H, Bloch W, Rösen P, Kelm M (2006) Red blood cells express a functional endothelial nitric oxide synthase. Blood 107:2943–2951. https://doi.org/10.1182/blood-2005-10-3992
57. Merx MW, Gorressen S, van de Sandt AM, Cortese-Krott MM, Ohlig J, Stern M, Rassaf T, Gödecke A, Gladwin MT, Kelm M (2014) Depletion of circulating blood NOS3 increases severity of myocardial infarction and left ventricular dysfunction. Basic Res Cardiol 109:398. https://doi.org/10.1007/s00395-013-0398-1
58. Liao R, Podesser BK, Lim CC (2012) The continuing evolution of the Langendorff and ejecting murine heart: new advances in cardiac phenotyping. Am J Physiol Heart Circ Physiol 303:H156–H167. https://doi.org/10.1152/ajpheart.00333.2012
59. Bell RM, Mocanu MM, Yellon DM (2011) Retrograde heart perfusion: the Langendorff technique of isolated heart perfusion. J Mol Cell Cardiol 50:940–950. https://doi.org/10.1016/j.yjmcc.2011.02.018
60. Paula TD, Silva BR, Grando MD, Souza HCD, Bendhack LM (2018) Activation of TP receptors induces high release of PGI2 in coronary arteries of renal hypertensive rats. J Mol Cell Cardiol 122:125–133. https://doi.org/10.1016/j.yjmcc.2018.08.007
61. Kane GC, Karon BL, Mahoney DW, Redfield MM, Roger VL, Burnett JC, Jacobsen SJ, Rodeheffer RJ (2011) Progression of left ventricular diastolic dysfunction and risk of heart failure. JAMA 306:856–863. https://doi.org/10.1001/jama.2011.1201
62. Avlas O, Fallach R, Shainberg A, Porat E, Hochhauser E (2011) Toll-like receptor 4 stimulation initiates an inflammatory response that decreases cardiomyocyte contractility. Antioxid Redox Signal 15:1895–1909. https://doi.org/10.1089/ars.2010.3728
63. Hill BGG, Dranka BPP, Zou L, Chatham JCC, Darley-Usmar VMM (2009) Importance of the bioenergetic reserve capacity in

response to cardiomyocyte stress induced by 4-hydroxynonenal. Biochem J 424:99–107. https://doi.org/10.1042/BJ20090934

64. Cimolai MC, Vanasco V, Marchini T, Magnani ND, Evelson P, Alvarez S (2014) Alpha-lipoic acid protects kidney from oxidative stress and mitochondrial dysfunction associated to inflammatory conditions. Food Funct 5:3143–3150. https://doi.org/10.1039/c4fo00489b
65. Boveris A, Carreras MC, Poderoso JJ (2010) The regulation of cell energetics and mitochondrial signaling by nitric oxide. In: Louise JI (ed) Nitric oxide biology and pathobiology, 2nd edn. pp 441–482. https://doi.org/10.1016/B978-0-12-373866-0.00013-7
66. Valdez LB, Bombicino SS, Iglesias DE, Rukavina Mikusic I, Boveris A (2018) Mitochondrial peroxynitrite generation is mainly driven by superoxide steady-state concentration rather than by nitric oxide steady-state concentration. Int J Mol Biol Open Access 3:56–61. https://doi.org/10.15406/ijmboa.2018.03.00051